British Journal of Pharmacology

DOI:10.1111/j.1476-5381.2011.01468.x
www.brjpharmacol.org

RESEARCH PAPER

Adrenoceptor activity of muscarinic toxins identified from mamba venoms

K Näreoja[1], JP Kukkonen[2,3], S Rondinelli[1], DM Toivola[4], J Meriluoto[1] and J Näsman[1]

[1]*Department of Biosciences, Biochemistry, Åbo Akademi University, Turku, Finland,* [2]*Department of Veterinary Biosciences, Biochemistry and Cell Biology, University of Helsinki, Helsinki, Finland,* [3]*Minerva Institute for Medical Research, Helsinki, Finland, and* [4]*Department of Biosciences, Cell biology, Åbo Akademi University, Turku, Finland*

Correspondence
Johnny Näsman, Department of Biosciences, Åbo Akademi University, Tykistökatu 6, FIN-20520 Turku, Finland.
E-mail: jonasman@abo.fi

Keywords
adrenoceptor; muscarinic toxin; receptor ligand; snake venom; three-finger toxin

Received
13 November 2010
Revised
30 March 2011
Accepted
21 April 2011

BACKGROUND AND PURPOSE

Muscarinic toxins (MTs) are snake venom peptides named for their ability to interfere with ligand binding to muscarinic acetylcholine receptors (mAChRs). Recent data infer that these toxins may have other G-protein-coupled receptor targets than the mAChRs. The purpose of this study was to systematically investigate the interactions of MTs with the adrenoceptor family members.

EXPERIMENTAL APPROACH

We studied the interaction of four common MTs, MT1, MT3, MT7 and MTα, with cloned receptors expressed in insect cells by radioligand binding. Toxins showing modest to high-affinity interactions with adrenoceptors were additionally tested for effects on functional receptor responses by way of inhibition of agonist-induced Ca^{2+} increases.

KEY RESULTS

All MTs behaved non-competitively in radioligand displacement binding. MT1 displayed higher binding affinity for the human α_{2B}-adrenoceptor (IC_{50} = 2.3 nM) as compared with muscarinic receptors ($IC_{50} \geq$ 100 nM). MT3 appeared to have a broad spectrum of targets showing high-affinity binding (IC_{50} = 1–10 nM) to M_4 mAChR, α_{1A}-, α_{1D}- and α_{2A}-adrenoceptors and lower affinity binding ($IC_{50} \geq$ 25 nM) to α_{1B}- and α_{2C}-adrenoceptors and M_1 mAChR. MT7 did not detectably bind to other receptors than M_1, and MTα was specific for the α_{2B}-adrenoceptor. None of the toxins showed effects on β_1- or β_2-adrenoceptors.

CONCLUSIONS AND IMPLICATIONS

Some of the MTs previously found to interact predominantly with mAChRs were shown to bind with high affinity to selected adrenoceptor subtypes. This renders these peptide toxins useful for engineering selective ligands to target various adrenoceptors.

Abbreviations

CCh, carbachol; HEL, human erythroleukaemia; mAChR, muscarinic acetylcholine receptor; MT, muscarinic toxin; NA, noradrenaline; NPY, neuropeptide Y

Introduction

G-protein-coupled receptors (GPCRs) constitute one of the largest known gene superfamilies with up to 750 members in humans (Vassilatis *et al.*, 2003). Because of this receptor diversity and the vast amount of physiological processes these receptors control or modulate, they are excellent targets for therapeutic interventions. Amongst the GPCRs, many families or subfamilies of receptors activated by the same endogenous substance exist; for example the classical neurotransmitter acetylcholine activates all five subtypes of muscarinic acetylcholine receptors (mAChRs) with

approximately equal potency (Caulfield and Birdsall, 1998). A classical enigma has been how to pharmacologically and therapeutically differentiate between such closely related subtypes within certain subfamilies of GPCRs, that is subtype-selective exogenous ligands have been very difficult to find from natural sources, or to synthesize chemically.

Many animals such as snakes, scorpions and marine snails have a diverse array of peptides in their venoms. These peptides have probably evolved to capture and immobilize preys or to be used in defense. Thus, many of the toxins interact with voltage-gated ion channels (Bosmans and Tytgat, 2007; Catterall *et al.*, 2007) and ligand-gated ion channels (Nirthanan and Gwee, 2004), ensuring a rapid paralysing action when used to envenom victims. Regarding toxins acting on GPCRs, the actual benefit of these for the animal is more difficult to predict. However, as shown on several occasions with ion channel-specific toxins, GPCR toxins may provide us with highly receptor subtype-selective tools and drug candidates. Amongst the first GPCR-acting toxins to be found were the muscarinic toxins (MTs) from the *Dendroaspis* genus of snakes (Adem *et al.*, 1988). The first two isolated toxins, MT1 and MT2, displaced radiolabelled quinuclidinyl benzilate from muscarinic receptors expressed in rat cortex in a way that suggested these toxins hold potential as subtype-selective ligands. Later studies showed that the toxins selectively targeted M_1 and M_4 of the mAChR family (Kornisiuk *et al.*, 1995a, b). The subtype-selectivity increased interest in these peptides and soon afterwards additional toxins MT3–MT7 were isolated from *Dendroaspis angusticeps* and MTα, MTβ, MTγ from *Dendroaspis polylepis*. All MTs are 65–66 amino acids long, and they all probably adopt a similar structure as α-neurotoxins with three loops or fingers held together by internal disulphide bonds (Ségalas *et al.*, 1995; Fruchart-Gaillard *et al.*, 2008).

MT3 and MT6, a probable isotoxin of MT3 for which the primary sequence has not been determined, show about 100-fold selectivity for M_4 receptors over M_1 receptors (Jolkkonen *et al.*, 1994; Karlsson *et al.*, 2000). MT7 (also called m1-toxin) appears to have absolute selectivity for the M_1 subtype with affinity values in the pico- to nanomolar range and lack of detectable binding to M_2–M_5 subtypes (Max *et al.*, 1993a; Näsman *et al.*, 2000; Mourier *et al.*, 2003). It is not known precisely how this selectivity is obtained at the structural level. Mutagenesis studies of MT7 suggest that all three fingers of the toxin are involved in the binding to the receptor (Fruchart-Gaillard *et al.*, 2008). Looking from the opposite side, the outer loops of the receptor, especially the second loop connecting transmembrane helices four and five, are important for toxin binding (Kukkonen *et al.*, 2004). The outer loops are usually less well conserved between subtypes of receptors in the rhodopsin-like GPCRs and may represent the structural elements required for high subtype selectivity of exogenous ligands.

Apart from their unusually high selectivity among muscarinic subtypes, the true specificity of MTs for mAChRs has occasionally been questioned (Bradley, 2000). In a study using MT1 and MT2 to show functional effects in different tissue preparations, Harvey *et al.* (2002) found that these toxins also interfered with adrenoceptor ligand binding. In a search for novel therapeutic agents for adrenoceptors, two new peptide toxins were recently found from *D. angusticeps* venom that showed high-affinity binding to α-adrenoceptors (Quinton *et al.*, 2010; Rouget *et al.*, 2010). The toxin ρ-Da1a appeared selective for the α_{1A}-adrenoceptor and ρ-Da1b displayed selective inhibition of the α_{2A}-adrenoceptor. We have recently reported on the high-affinity binding of MTα to the α_{2B}-adrenoceptor (Koivula *et al.*, 2010). Using synthetic MTα, we found this toxin had no muscarinic receptor activity in contrast to what has previously been reported for the venom-derived toxin (Jolkkonen *et al.*, 1995b). In this study, we have continued our screening of known MTs for adrenoceptor activity, and we now report that MT1 and MT3 display prominent adrenoceptor activity in addition to muscarinic receptor activity, whereas MT7 and MTα seem restricted to their single target receptors.

Methods

Test systems used

Spodoptera frugiperda Sf9 cells were grown in suspension at 27°C in Grace's insect medium (Invitrogen, Paisley, UK) supplemented with 8% fetal bovine serum (Invitrogen), 50 $\mu g \cdot mL^{-1}$ streptomycin (Invitrogen), 50 $U \cdot mL^{-1}$ penicillin (Invitrogen) and 0.02% Pluronic F68 (Sigma-Aldrich, Helsinki, Finland). Human erythroleukaemia (HEL) cells were grown in RPMI 1640 medium (Lonza, Verviers, Belgium) supplemented with 10% fetal bovine serum (Invitrogen), 1% penicillin-streptomycin stock (Invitrogen) and 2 mM glutamine (Invitrogen). Cells were maintained at 37°C in 95% air: 5% CO_2 atmosphere.

The human α_1-adrenoceptor cDNAs were kind gifts from Dr K Minneman (Emory University School of Medicine, Atlanta, GA). Baculovirus-mediated expression of the human α_{1A}- and α_{1B}-adrenoceptors (Koivula *et al.*, 2010), α_2-adrenoceptors (Oker-Blom *et al.*, 1993; Jansson *et al.*, 1995) and mAChRs (Kukkonen *et al.*, 1996; Näsman *et al.*, 2000) in Sf9 cells has been described previously. In this study, new baculovirus vectors for all of these receptors and the α_{1D}-adrenoceptor were made to include a Rous sarcoma virus promoter, which we have found to enhance the expression of receptors in this system as compared with the polyhedrin promoter (the details of this will be described elsewhere). The cDNA for the human β_1-adrenoceptor was a kind gift from Dr S Uhlén (Institute of Medicine, University of Bergen, Bergen, Norway), and human β_2-adrenoceptor cDNA was purchased from Missouri S&T cDNA Resource Center (Rolla, MO). The β-adrenoceptor cDNAs were subcloned into FastBac1 and baculovirus generated with the Bac-to-Bac system (Invitrogen).

Sf9 cells aimed for membrane preparations were infected with receptor virus in batches of 80 mL (2×10^6 $cells \cdot mL^{-1}$) in suspension cultures for 48–72 h, whereafter harvested by centrifugation, washed once with cold PBS and stored as pellets at –70°C. For the functional assay, cells were seeded on tissue culture dishes and infected with receptor virus for 26–28 h. In the case of co-expression of $G_{11}\alpha i5$ (Kukkonen *et al.*, 2004) and receptor, which was required for the G_i-coupled M_4 mAChR and α_{2A}- and α_{2C}-adrenoceptors in measurements of intracellular Ca^{2+} increases, the cells were first infected with the chimeric G-protein construct for 30 min and then with

the receptor virus for another 30 min before exchange to fresh medium.

Membrane preparations and buffer compositions

Crude membrane fractions of infected Sf9 cells and HEL cells were obtained by resuspending the thawed cell pellets in the buffer solution (same solutions as used for the binding experiments; see below) and homogenizing using a T25 Ultra-Turrax homogenizer (IKA, Staufen, Germany). The solutions were then subjected to low speed centrifugation and the supernatants centrifuged 30 000× *g* for 45 min at 4°C. The pelleted membranes were washed once in buffer, resuspended in buffer (1–3 mg protein·mL^{-1}) and stored at –70°C. Protein concentrations were determined using the Bio-Rad protein assay (Bio-Rad Laboratories, Hercules, CA, USA) with BSA as standards. The buffers used in the preparations and in the binding assays were 20 mM Tris, 1 mM EDTA, 5 mM $MgCl_2$, pH 7.4 for α_1- and β-adrenoceptors; 25 mM $NaPO_4$, pH 7.4 for α_2-adrenoceptors; 100 mM NaCl, 20 mM HEPES, 10 mM $MgCl_2$, 1 mM EDTA, pH 7.4 for mAChRs.

Adult female Sprague–Dawley rats were killed by carbon dioxide inhalation, and the kidneys and whole brain excised and immediately frozen at –70°C. After being thawed, the tissues were cut into pieces in buffer and homogenized with a Potter–Elvehjem glass homogenizer. For the brain tissue, we used a buffer containing 0.32 M sucrose, 10 mM HEPES, 2 mM EDTA, pH 7.4 and for the kidney a buffer containing 50 mM Tris, 1 mM EDTA, pH 7.4, both buffers supplemented with a protease inhibitor cocktail (Complete™, Roche Diagnostics GmbH, Mannheim, Germany). Low-speed centrifugations of the homogenates were done at 1000× *g* for 10 min, after which the supernatants were centrifuged 30 000× *g* for 45 min. The pellets were resuspended in 50 mM Tris, 1 mM EDTA, pH 7.4 at 3–5 mg protein·mL^{-1} and stored at –70°C.

Radioligand binding assays

Prior to radioligand binding experiments, the membrane preparations were thawed on ice and diluted to appropriate volumes. To determine the K_d and B_{max} values of receptors with their respective radioligand, 15–50 µg of cell membranes were incubated with various concentrations of radioligand (0.1–30 nM [^{3}H]-prazosin, 0.1–10 nM [^{3}H]-MK-912, 0.1–30 nM [^{3}H]-CGP-12177, 0.1–10 nM [^{3}H]-NMS) in a total volume of 150 µL for 90 min with shaking at room temperature. Non-specific binding was determined in the presence of 10–100 µM phentolamine (α_1- and α_2-adrenoceptors), 10 µM propranolol (β-adrenoceptors) or 10 µM atropine (mAChRs). In displacement studies, the receptors were first pre-incubated for 30 min with different concentrations of toxins in 100 µL, after which radioligand in 50 µL was added to the receptors for another 60 min. The concentrations of toxins used in the calculations were always the concentrations present in the final 150 µL volumes. Unless otherwise stated, the concentration of radioligand was 1 nM for adrenoceptors and 0.5 nM for mAChRs in the displacement binding experiments.

To determine the radioligand dissociation rate, receptors were first incubated with 1.5 nM radioligand for 45 min, and thereafter dissociation was initiated by the addition of 1 µM phentolamine (α_1- and α_2-adrenoceptors) or 10 µM atropine (mAChRs). Samples were withdrawn at different time points and bound radioactivity determined. When the effect of MT was tested, the toxin was included in the dissociation initiator solution.

All reactions were terminated by rapid filtration through prewashed GF/B filters (PerkinElmer, Waltham, MA). Filter plates were then washed five times with cold wash buffer containing 180 mM NaCl, 25 mM $MgCl_2$ and 20 mM HEPES, pH 7.4 in a microplate harvester (PerkinElmer). Radioactivity bound to the filters was determined in a microplate scintillation counter (PerkinElmer).

Measurement of intracellular [Ca^{2+}]

Infected Sf9 cells were detached from culture dishes and incubated for 20 min with 4 µM fura-2 acetoxymethyl ester in culture medium. After this, cells were diluted two times with culture medium and kept at room temperature in the dark. For fluorescence recordings, an aliquot of the cells was spun down and washed twice in assay buffer [129.7 mM NaCl, 5.44 mM KCl, 1.2 mM $MgCl_2$, 4.2 mM $NaHCO_3$, 7.3 mM NaH_2PO_4, 1 mM $CaCl_2$, 20 mM 2-(*N*-morpholino)ethanesulphonic acid (MES), 10 mM glucose, 63 mM sucrose, pH adjusted to 6.3]. After the final resuspension in assay buffer, the cells were transferred into a thermostatted (27°C) cuvette with magnetic stirring in a Hitachi F-2000 fluorescence spectrophotometer. Recordings at 340 nm (excitation) and 505 nm (emission) were briefly interrupted for additions of agonists and toxins, and at the end calibrated using 0.04% Triton X-100 to obtain F_{max} and 10 mM EGTA to obtain F_{min}. Intracellular calcium concentrations were calculated according to the equation $[Ca^{2+}] = (F - F_{min}) / (F_{max} - F) \times K_d$ for the fura-2–Ca^{2+} complex (255 nM at 27°C) (Shuttleworth and Thompson, 1991).

When MTs were included in the experiments, the toxins were allowed to bind to receptors for 2–3 min prior to agonist additions in the short-term incubation experiments. For longer times of toxin incubations (≥60 min), the cells were kept in culture medium with the toxin and then treated as above in the constant presence of the toxin.

HEL cells were detached from the 75 cm^2 culture bottles by gentle shaking, centrifuged, resuspended in culture medium and loaded with 4 µM fura-2 acetoxymethyl ester for 20 min.

After this, the cells were spun down and washed once in assay buffer (137 mM NaCl, 5 mM KCl, 0.44 mM KH_2PO_4, 4.2.mM $NaHCO_3$, 20 mM HEPES, 10 mM glucose, 1 mM $CaCl_2$, 1.2 mM $MgCl_2$, pH adjusted to 7.4), resuspended in assay buffer, divided into aliquots and kept at 37°C in the dark. Fluorescence measurements were done as described for Sf9 cells except for the temperature, which was 37°C in the cuvette holder. The K_d of 224 nM was used in the calculation of the Ca^{2+} concentration.

Data analysis

All data analyses were done using GraphPad Prism (GraphPad Software, San Diego, CA). Non-linear curve fitting was used to determine K_d and B_{max} values. IC_{50} values in displacement studies were determined using the equation

$$B = B_{min} + \frac{B_{max} - B_{min}}{1 + 10^{\log[I] - \log IC_{50}}},$$

which is a log-form of the classical

$$B = B_{min} + \frac{B_{max} - B_{min}}{1 + \frac{[I]}{IC_{50}}}$$

where B is the bound radioligand and [I] is the concentration of toxin (inhibitor) in the sample.

In functional inhibition experiments with toxins, the apparent inhibitory constants were obtained by curve-fitting to the equation:

$$\Delta[Ca^{2+}] = \frac{[A] \times \Delta[Ca^{2+}]_{max}}{[A] + EC_{50}}$$

where $\Delta[Ca^{2+}]$ is the cellular increase in Ca^{2+} concentration, [A] the concentration of agonist, respectively, and EC_{50} the [A] producing half-maximal stimulation. In cases where the toxin also caused depression of the maximum response (insurmountable inhibition), the maximum response ($\Delta[Ca^{2+}]_{max}$) was fitted accordingly. The apparent K_i values were derived from the shift according to:

$$EC_{50,toxin} = \left(1 + \frac{[I]}{K_i}\right) EC_{50,ctrl} \Leftrightarrow K_i = \frac{EC_{50,ctrl}}{EC_{50,toxin} - EC_{50,ctrl}} \times [I]$$

where [I] is the concentration of the inhibitor. Each K_i value was derived using several toxin concentrations and thus the apparent pK_i values reported correspond to the pA_2 values from Schild analysis (for inhibitors displaying pure surmountable inhibition).

Materials

Synthetic MTα, MT1 and MT3 were from Peptide Institute (Osaka, Japan). MT7 was recombinantly expressed and purified as previously described (Näsman *et al.*, 2000). Noradrenaline bitartrate, carbachol, atropine hemisulphate and neuropeptide Y (NPY) were from Sigma-Aldrich. UK-14,304 [5-bromo-*N*-(4,5-dihydro-1*H*-imidazol-2-yl)-6-quinoxalineamine] and phentolamine hydrochloride were from RBI (Natick, MA). Propranolol was from Tocris Biosciences (Bristol, UK). Fura-2 acetoxymethyl ester was from Molecular Probes (Eugene, OR). [^{3}H]-MK-912 [(2*S*,12b*S*)1′,3′-dimethylspiro(1,3,4,5′,6,6′,7,12b-octahydro-2*H*-benzo[b]furo[2,3a]quinolizine)-2,4′-pyrimidin-2′-one, specific activity 79.1 Ci·mmol^{-1}], [^{3}H]-prazosin [2-[4-(2-furoyl)piperazin-1-yl]-6,7-dimethoxyquinazolin-4-amine, specific activity 85.3 Ci·mmol^{-1}], [^{3}H]-CGP-12177 [(−)-4-(3-*tert*-butylamino-2-hydroxypropoxy)-[5,7-*H*]benzimidazol-2-one, specific activity 30.0 Ci·mmol^{-1}] and [^{3}H]-NMS (*N*-methyl scopolamine, specific activity 82.0 Ci·mmol^{-1}) were from PerkinElmer.

Results

Receptor expression

In order to study the effect of toxins on receptors, we expressed the adrenoceptors and muscarinic receptors in Sf9 cells (Table 1). The muscarinic receptors and the α_2-adrenoceptors have been used for many years with this expression system for the characterization of MT action (Näsman *et al.*, 2000; Koivula *et al.*, 2010). The α_{1A}- and α_{1B}-adrenoceptors were recently expressed and characterized functionally by measuring the noradrenaline-induced Ca^{2+} responses (Koivula *et al.*, 2010). In the present study, we used radiolabelled prazosin to further characterize the α_1-adrenoceptors. We also managed to obtain reasonable expression of the α_{1D}-adrenoceptors by manipulating with the transcriptional promoters in the virus constructs. The K_d and B_{max} values for different receptors determined with their respective radioligand are listed in Table 1. All K_d values are in general agreement with previously reported affinity values obtained in other expression systems (Uhlen *et al.*, 1998; Williams *et al.*, 1999; Baker, 2005). MK-912, which is selective for the α_{2C} subtype, also displays high affinities for the α_{2A}- and α_{2B}-adrenoceptors and is thus very useful when studying heterologously expressed receptors.

The binding of the toxins used here to mAChRs has previously been analysed in many different laboratories (reviewed in Bradley, 2000; Karlsson *et al.*, 2000; Servent and Fruchart-Gaillard, 2009). The M_1 and M_4 subtypes were included in this study, because MT1 and MT3 have not been tested previously in the experimental setup of our laboratory, and these receptor subtypes also served as positive controls for MT1, MT3 and MT7.

Table 1
Radioligand binding data for expressed receptors

Receptor	^{3}H-ligand K_d (pM)	B_{max} (fmol mg^{-1} protein)
Adrenoceptor		
	[^{3}H]-prazosin	
α_{1A}	234 ± 31	2191 ± 53
α_{1B}	181 ± 28	1946 ± 59
α_{1D}	148 ± 31	438 ± 18
	[^{3}H]-MK-912	
α_{2A}	876 ± 128	5190 ± 141
α_{2B}	599 ± 134	10343 ± 409
α_{2C}	86 ± 32	1101 ± 186
	[^{3}H]-CGP-12177	
β_1	664 ± 189	2910 ± 249
β_2	738 ± 204	2385 ± 204
mAChR	[^{3}H]-NMS	
M_1	460 ± 78	3162 ± 115
M_4	190 ± 34	888 ± 35

Saturation binding experiments were performed using crude membrane preparations of infected Sf9 cells. Data are mean values ± SD from one batch of membranes analysed in two separate experiments.

Radioligand displacement studies

MT1 is one of the best-studied MTs, with selective binding to the M_1 and M_4 subtypes of mAChRs (Kornisiuk *et al.*, 1995a,

b; Mourier *et al.*, 2003). In displacement studies with the α_{2B}-adrenoceptor, MT1 inhibited the [^{3}H]-MK-912 binding with an IC_{50} of 2.3 nM (Figure 1, Table 2). The toxin binding behaved non-competitively as judged from the inability to completely displace bound radioligand. A similar IC_{50} value was obtained with MTα (Table 2), in agreement with the IC_{50} value (3.2 nM) we reported previously in competition with [^{3}H]-RX821002 (K_d = 3.3 nM) (Koivula *et al.*, 2010). In accordance with its role as a muscarinic toxin, MT1 also displaced [^{3}H]-NMS from M_1 and M_4 mAChRs (Table 2). Interference with [^{3}H]-prazosin binding could be detected on each α_1 subtype with the highest affinity determined for the α_{1A}-adrenoceptor. For receptors binding with low affinities, we chose to indicate % inhibition obtained with 1 μM toxin since the inhibition curves did not reach saturation at the concentrations used (Table 2). The usual pattern found for these titrations is exemplified by the α_{2A}-adrenoceptor in Figure 1.

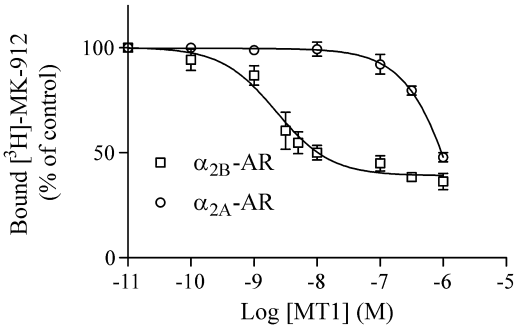

Figure 1

Cellular membranes with α_{2A}- or α_{2B}-adrenoceptors were incubated with different concentrations of MT1 and 1 nM [^{3}H]-MK-912 for a total of 90 min, after which the samples were filtrated to remove unbound ligands and then subjected to scintillation counting. Data points are given as % of control binding and represent means ± SEM of three experiments each performed with triplicate samples. The pIC_{50} value for the saturating inhibition was determined with computational fitting (Table 2). The data with the α_{2A}-adrenoceptor serve as an example of inhibitory potencies when given as % inhibition in Table 2.

The synthetic MT3 exhibited much higher affinity for the M_4 subtype than for the M_1 mAChR, as previously found for the venomous MT3 (Jolkkonen *et al.*, 1994; Liang *et al.*, 1996). Surprising was the high-affinity displacement we found with several adrenoceptor subtypes. MT3 was equally potent at the α_{1A} and only slightly less potent at α_{1D} and α_{2A} as compared with the M_4 subtype (Figure 2, Table 2). Relatively high affinity was also found for the α_{1B} and α_{2C} subtypes (Table 2). In all displacements obtaining saturating inhibitions with MT3, the non-competitive nature of binding was prevailing. The non-competitivity was also tested by using different radioligand concentrations. As exemplified in Figure 3 for the α_{1A}-adrenoceptor and MT3, there were no obvious shifts in the IC_{50} values, which would be expected if the ligands competed for the same binding site. MT3 behaved similarly at the α_{2A}-adrenoceptor (Figure 3C) and at the α_{1D}- and α_{2C}-adrenoceptors when loaded with different radioligand concentrations (0.3 and 1 nM; data not shown). For the M4 receptor, the inhibition curve shifted as for competitive interactions when going from 0.5 to 1.5 nM radioligand, but no further shift was seen with 5 nM (Figure 3C).

Allosteric effects on orthosteric ligand dissociation have sometimes been implicated in MT action (Max *et al.*, 1993b; Mourier *et al.*, 2003; Olianas *et al.*, 2004). Because MT3 bound to several receptors with high affinity, we aimed to look for potential differences in the interaction of MT3 with its multiple targets. MT3 did not, however, show any effect on the dissociation rates of radioligands from α_{1A}, α_{2A} or M_4 receptors (Table 3), indicating that the toxin does not allosterically

Table 2

MT inhibition profiles at different receptors

Receptor	pIC_{50} ±SEM (n = 3–4) MT1	MT3	MT7	MTα
α_{1A}	6.98 ± 0.17	8.86 ± 0.14	NI	NI
α_{1B}	<6.5 (48%)[a]	7.57 ± 0.22	NI	NI
α_{1D}	<6 (28%)[a]	8.13 ± 0.08	NI	NI
α_{2A}	<6.5 (47%)[a]	8.49 ± 0.06	NI	NI
α_{2B}	8.64 ± 0.10	<6.5 (39%)[a]	NI	8.62 ± 0.12
α_{2C}	NI	7.29 ± 0.13	NI	NI
β_1	NI	NI	NI	NI
β_2	NI	NI	NI	NI
M_1	6.85 ± 0.06	6.71 ± 0.14	9.36 ± 0.06[b]	NI
M_4	6.54 ± 0.09	8.79 ± 0.06	NI	NI

The inhibitory potencies of different MTs were determined in radioligand displacement experiments.
[a]% values in parentheses indicate inhibition with 1 μM toxin.
[b]Analysis of the dissociation kinetic of [^{3}H]-NMS in relation to MT7 concentrations resulted in $pIC_{50,\ diss}$ = 8.31 ± 0.04.
NI, no inhibition. The threshold for inhibition was set to 25% at 1 μM concentration for MT1, MT3 and MTα and 0.3 μM for MT7.

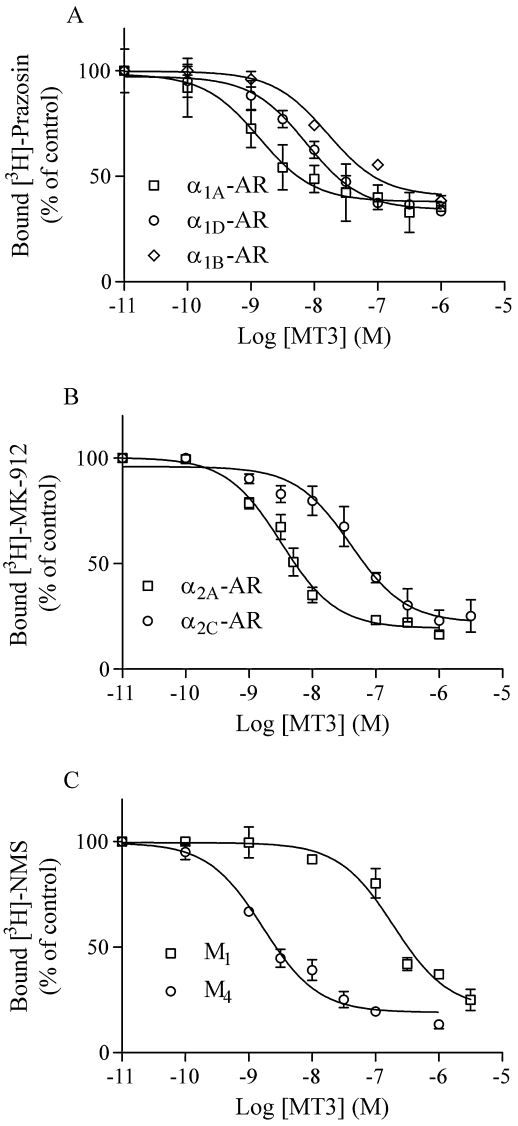

Figure 2

Different receptors expressed in membranes of Sf9 cells were subjected to MT3 displacement binding of [^{3}H]-prazosin for α_1-adrenoceptors (A), [^{3}H]-MK-912 for α_2-adrenoceptors (B) and [^{3}H]-NMS for mAChRs (C). Sample and data processing were as in Figure 1. Data points are means ± SEM of three experiments performed in triplicate.

alter antagonist dissociation or obstruct the exit of the antagonist by steric hindrance at the entrance of the ligand binding cavity.

Functional inhibition

In general, the MTs behave as antagonists of receptor responses. MT2 could be an exception to this rule, based on the toxin-induced cytosolic Ca^{2+} increases reported with CHO cells expressing different mAChRs (Bradley *et al.*, 2003). MT1 has also been implicated in agonistic actions using functional output from different tissue preparations (Jerusalinsky *et al.*, 1995; Jolkkonen *et al.*, 1995a; Harvey *et al.*, 2002). We tested the effect of MT1 on the α_{2B}-adrenoceptor and M_1 mAChR by monitoring the receptor-activated Ca^{2+} response in Sf9 cells. In the concentration range of 10–300 nM, acute application of MT1 did not elicit any response from either receptor (data not shown). Instead, the responses to the agonists noradrenaline and carbachol, respectively, were inhibited. In our previous work, we have noticed that it may be necessary to incubate receptors with toxin for a considerable time (>30 min) before stimulating with agonist to reveal the true antagonistic potencies of toxins (Koivula *et al.*, 2010). We therefore pre-incubated cells for ≥60 min with different concentrations of MT1 and measured the agonist responses (Figure 4 and Table 4). MT1 behaved very similarly to MTα on the α_{2B}-adrenoceptor (Koivula *et al.*, 2010), with a pronounced insurmountable inhibition of the response. On the M_1 receptor, MT1 inhibited the response surmountably with an apparent K_i of 35 ± 11 nM (mean ± SD, n = 4). A low concentration of the M_1-selective MT7 was included in the same assay for comparison with the more complex inhibition pattern produced by this toxin on the M_1 receptor (Figure 4B).

MT3 is a well-characterized mAChR antagonist with a pA_2 value of 8.33 derived from functional inhibition of cloned M_4 receptors (Olianas *et al.*, 1999). To further explore its action on the adrenoceptors, we performed functional Ca^{2+} assays with the different high-affinity targets (Figure 5). For these, we analysed the responses both after short (2–3 min) and long (≥60 min) pre-incubations with MT3. Potential responses due to toxin applications were monitored in the short-term experiments to reveal agonistic effects, but none was found. The responses with control cells without toxin did not generally change during the time windows used, and if so, the experiments were discarded. In the long-term incubations, we did not observe further inhibition of any receptor from 60 min up to 120 min (data not shown), indicating that the binding of toxin reached equilibrium within 60 min.

Short pre-incubations with toxins may not be adequate to observe an effect on receptor responses, as shown in Figure 5. This slow binding was most pronounced for the α_{2A}-adrenoceptor (Figure 5D), where there was no obvious effect even with 100 nM MT3, despite the high affinity determined in radioligand binding experiments. The inhibitory potency of MT3 became obvious though with a long pre-incubation time. Another important observation we made, as regards interpretation of toxin binding modes from functional receptor analyses, was the effect of MT3 on the α_{1A}-adrenoceptor. In Figure 5A the analyses of responses using cells expressing a relatively high density of receptors (1350 ± 160 fmol mg^{-1} protein of homogenized cells, mean ± SD, n = 3) are plotted. Long pre-incubations with 30 nM MT3 did not show any insurmountable effect. In Figure 5B, the same type of experiments were performed with cells expressing the same α_{1A}-adrenoceptor cDNA, but at a much lower density (59 ± 10 fmol mg^{-1} protein of homogenized cells, mean ± SD, n = 3). With these cells, the response was strongly depressed with 30 nM MT3. Our interpretation of these data is that a receptor reserve exists in the high-expressing cells, and therefore, the non-occupied receptor population can still elicit a full response. The almost 100-fold difference in the potency for noradrenaline with control cells from these two expression levels points towards a similar interpretation. However, using

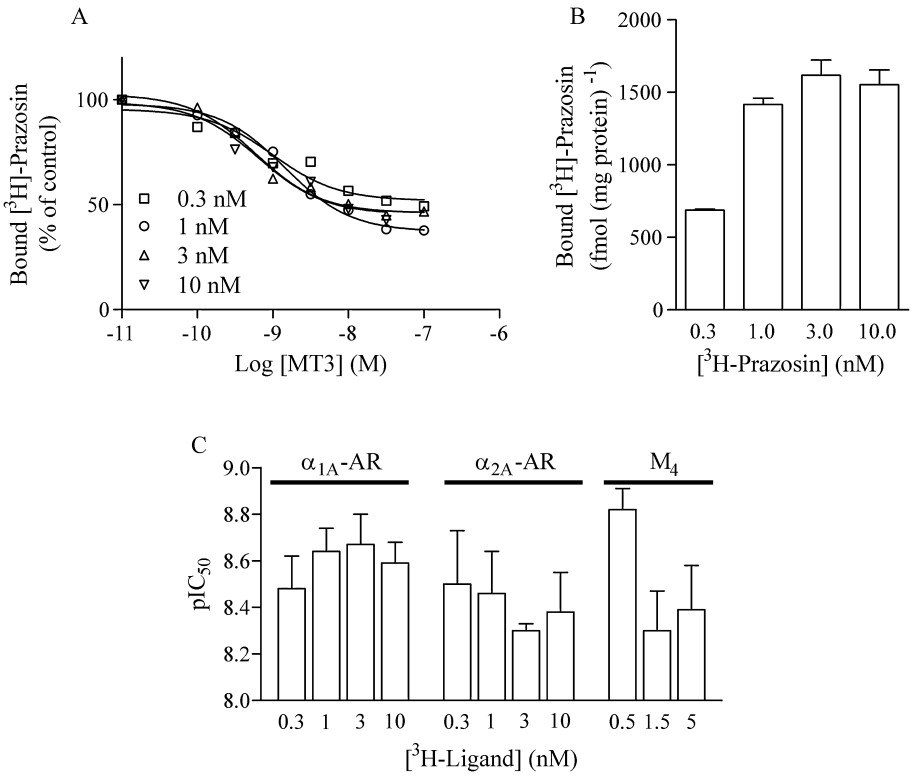

Figure 3

The inhibitory potency of MT3 was tested on α_{1A}-adrenoceptor membranes in the presence of different concentrations of [^{3}H]-prazosin (A). Sample and data processing were as in Figure 1. All data points are from one experiment performed using the same membrane preparation, and plotted as means of triplicate samples. (B) The control binding for α_{1A}-adrenoceptor expressed in fmol·(mg of protein)$^{-1}$ (means ± SD, $n = 3$) with different concentrations of [^{3}H]-prazosin. (C) pIC_{50} values plotted as a function of radioligand concentrations for α_{1A}, α_{2A} and M_4 mAChR. Values are means ± SEM ($n = 3$) from fitted curves.

Table 3

Dissociation rate constants for the radioligands [^{3}H]-prazosin (α_{1A}), [^{3}H]-MK-912 (α_{2A}) and [^{3}H]-NMS (M_4)

Receptor	[^{3}H]-Ligand dissociation rate (min^{-1}) Control	30 nM MT3	300 nM MT3
α_{1A}	0.0400 ± 0.0024	0.0441 ± 0.0024	0.0403 ± 0.0050
α_{2A}	0.0264 ± 0.0024	0.0273 ± 0.0026	0.0328 ± 0.0089
M_4	0.0271 ± 0.0054	0.0268 ± 0.0051	0.0287 ± 0.0068

Data are given as means ± SD from two experiments.

lower concentrations of MT3 to assess the potency of the toxin with the low-expressing α_{1A}-adrenoceptor gave a similar apparent pK_i value as with the high-expressing cell batch (Table 4). Overall, the relative potencies (pK_i values) of the toxin, determined from the inhibited responses of the different receptors, followed quite closely the relative potencies (pIC_{50} values) found in the displacement binding (Tables 2 and 4).

Native receptor inhibition by MTs

The HEL cell line has been used by several laboratories to study the intracellular Ca^{2+} dynamics elicited through α_2-adrenoceptors (Michel *et al.*, 1989; Musgrave and Seifert, 1995; Kukkonen *et al.*, 1997). Pharmacological data indicate that the α_{2A} subtype is endogenously expressed in these cells. To confirm the effect of MT3 on endogenously expressed α_{2A}-adrenoceptors, we pre-incubated the cells with 100 nM MT3 for 60 min and measured the responses. This concentration of MT3 totally blocked the response to 100 nM UK14,304, an α_2-adrenoceptor agonist (Figure 6A). The response to NPY, through the activation of endogenous NPY receptors, did not change with MT3. In the radioligand displacement assay, MT3 inhibited [^{3}H]-MK-912 binding with a

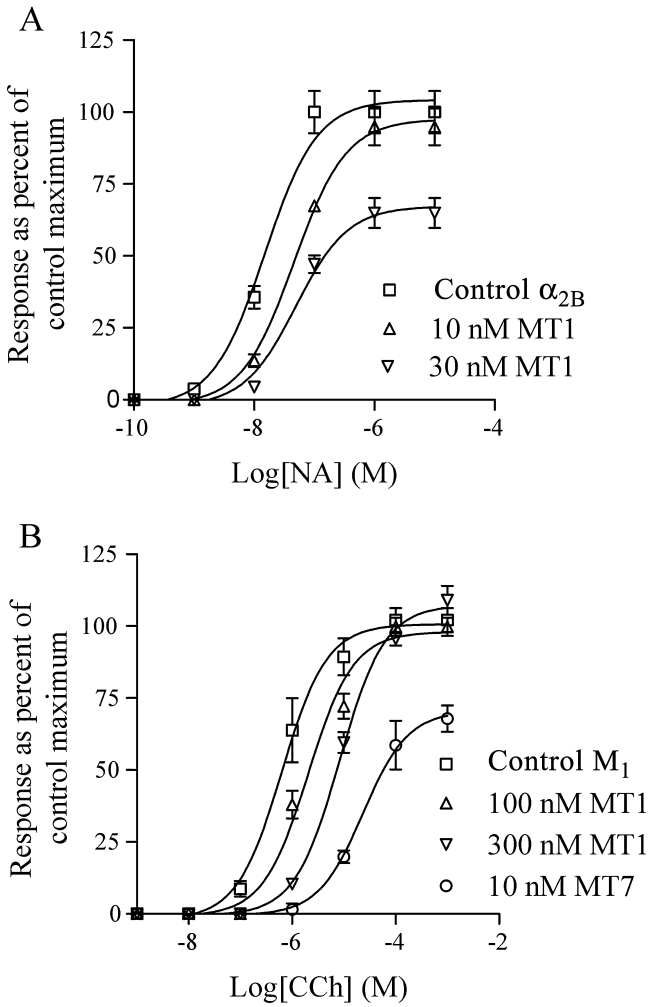

Figure 4

Sf9 cells expressing the α_{2B}-adrenoceptor (A) or M_1 mAChR (B) were loaded with fura-2 and subjected to fluorescence recordings to measure intracellular [Ca^{2+}] levels. Different concentrations of toxins were added to aliquots of cells and incubated for ≥60 min. Control cells were treated similarly with vehicle. Noradrenaline (NA) and carbachol (CCh) were used to stimulate the α_{2B} and M_1 receptors, respectively. Data points (means ± SD, n = 3–5) are given as % of control maxima. The absolute response maxima varied somewhat between days of experimentation. For α_{2B}-AR, the response maxima were in the range 570–743 nM and for M_1 in the range 214–254 nM. Data for MT7 were included for comparison with the effect of a toxin with high affinity binding to the M_1 receptor.

pIC_{50} = 8.65 ± 0.20, confirming its potency also for the native human α_{2A}-adrenoceptor (Figure 6B).

Because we could not find appropriate human cell lines to test native α_1- and α_{2B}-adrenoceptor binding, we used rat tissues to verify the toxin effects. Whole rat brain membranes were labelled with [^{3}H]-prazosin and analysed for displacement by MT3. The pIC_{50} for MT3 was 8.85 ± 0.07 with this preparation (Figure 6C). A similar pIC_{50} (8.50 ± 0.18) was found for [^{3}H]-prazosin-labelled kidney membranes (Figure 6C). To test MT binding on α_{2B}-adrenoceptors, we used rat kidney membranes. The kidney tissue is a known source of α_{2B}-adrenoceptors (Huang *et al.*, 1996), and the [^{3}H]-MK-912-labelled sites of this organ were potently displaced by MT1 (pIC_{50} = 9.01 ± 0.11) and by MTα (pIC_{50} = 8.76 ± 0.08) (Figure 6D).

Table 4

Apparent affinity constants for MT inhibition of receptor-stimulated Ca^{2+} increases

Receptor	Apparent pK_I
MT1	
α_{2B}	8.28 ± 0.38
M_1	7.47 ± 0.13
MT3	
α_{1A} (high)	9.19 ± 0.13
α_{1A} (low)	8.74 ± 0.23
α_{1D}	8.28 ± 0.05
α_{2A}	8.20 ± 0.32
α_{2C}	7.92 ± 0.11
M_4	8.50 ± 0.18

Analyses were done with two or three different concentrations of toxin and the values represent means ± SD from three to six experiments.

Discussion

The present study confirms the specificity of MT7 for the M_1 mAChR and the specificity of synthetic MTα for the α_{2B}-adrenoceptor, with reservations for the activity of venomous MTα, which has not been thoroughly investigated (Koivula *et al.*, 2010). In contrast to these toxins, MT1 and MT3 exhibited a somewhat unexpectedly broad range of receptor targets among the adrenoceptors. Some of the α-adrenoceptors were found to bind these toxins with high affinities, and MT1 actually bound more tightly to the α_{2B}-adrenoceptor than to the previously identified muscarinic targets. No activity of the tested toxins was detected on the β-adrenoceptors. This could indicate that the β-adrenoceptors are structurally very different from the α-adrenoceptors in terms of MT binding. A hint of such a structural difference could emanate from the folding of the second extracellular receptor loop, which in β-adrenoceptors contains two disulphide bridges that constrain the loop folding more than in the α-adrenoceptors that contain only one such bridge (Cherezov *et al.*, 2007). Nevertheless, the structurally related β-cardiotoxin found from the king cobra shows β-adrenoceptor activity (Rajagopalan *et al.*, 2007), suggesting that snake venoms could be a source of subtype-selective β-adrenoceptor ligands as well.

The primary sequences of MT1 and MTα are very similar (Table 5). Of the four different residues, three are clustered near the tip of the middle finger, that is $I^{31}VP^{33}$ in MT1 and $L^{31}NH^{33}$ in MTα. The tip of the middle finger, in general a basic residue, R^{34} or K^{34} in MTs, is believed to reach down into the orthosteric binding cleft and to interact with transmem-

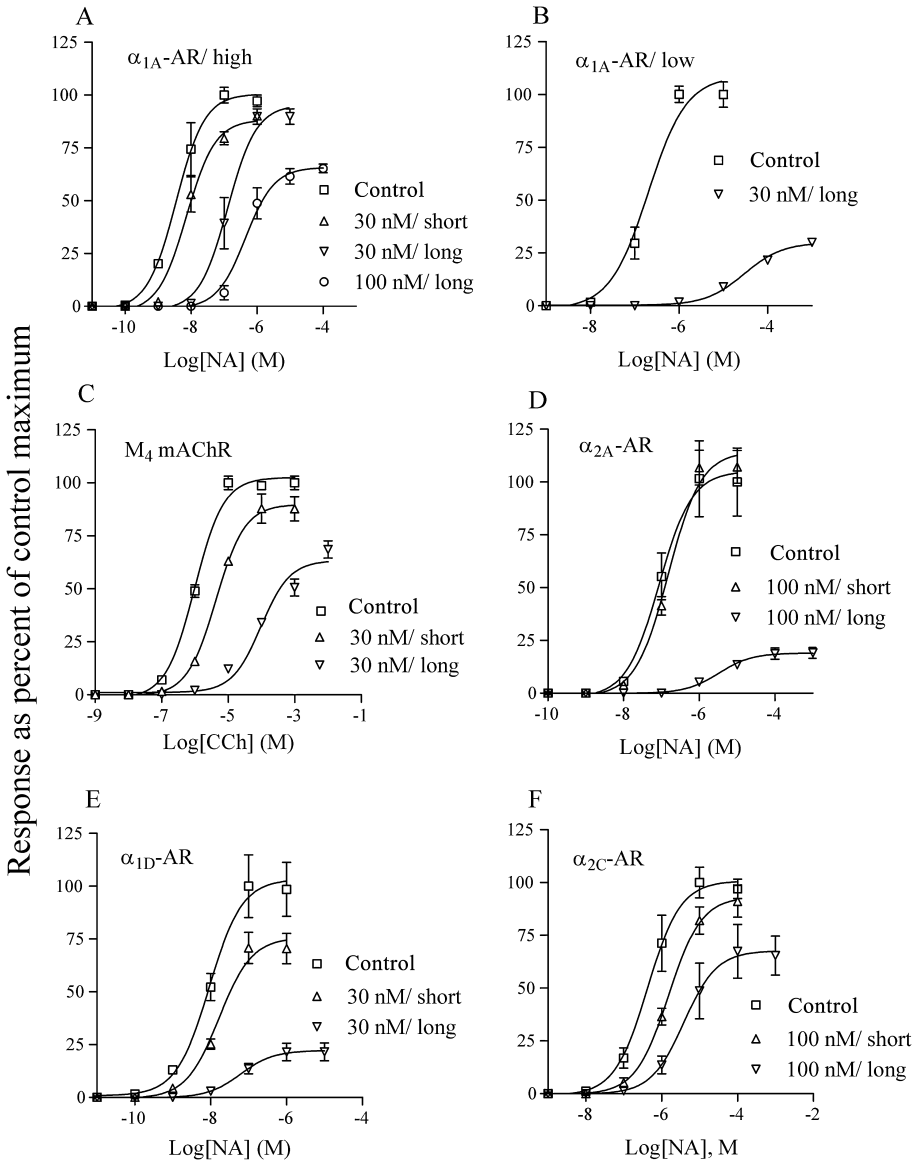

Figure 5

Cellular [Ca^{2+}] responses were measured in Sf9 cells expressing the α_{1A} (A and B; high receptor expression in A and low in B), M_4 mAChR (C), α_{2A} (D), α_{1D} (E) and α_{2C} (F). Different concentrations of MT3 were added to aliquots of cells and pre-incubated for 2–3 min (short) or ≥60 min (long) before being stimulated with agonist. Control cells were treated similarly with vehicle. Data points (means ± SD, n = 3–6) are given as % of control maxima. The ranges for the response maxima were (in nM): 595–855 (A), 526–572 (B), 576–728 (C), 526–803 (D), 662–978 (E), 299–528 (F).

brane helix residues of the receptor (Ségalas *et al.*, 1995). The adjacent residues on both sides of the finger would thus be in such positions that they could interact with the outer surface of the receptor. Our hypothesis was that the LNH cluster of MTα could be an α_{2B} recognition motif. However, since MT1 was found to bind equally well to the α_{2B}-adrenoceptor as MTα, such a restricted motif probably does not exist. On the other hand, the LNH sequence of MTα appears to prevent this toxin from binding to the muscarinic receptors and thereby fulfills a specific function from a pharmacological point of view. The fourth difference in the sequences between MT1 and MTα, R^{57} and H^{57} is located adjacent to the disulphide bridge making up the third finger of the toxin. It is likely that this substitution does not play a significant role in binding selection because MT4, which differs from MT1 only at position H^{57}, binds to M_1 and M_4 receptors with similar affinities as MT1 (Vandermeers *et al.*, 1995; Karlsson *et al.*, 2000). It is therefore also likely that MT4 is an antagonist with higher affinity for the α_{2B}-adrenoceptor than for muscarinic receptors. The influence of side chain differences at residue 57 could be rigorously tested with MT4 when synthesized.

MT1 antagonized the responses of α_{2B} in the functional assay. Characteristic for the toxins that binds with high affinity to the receptors in this type of assays is the insurmount-

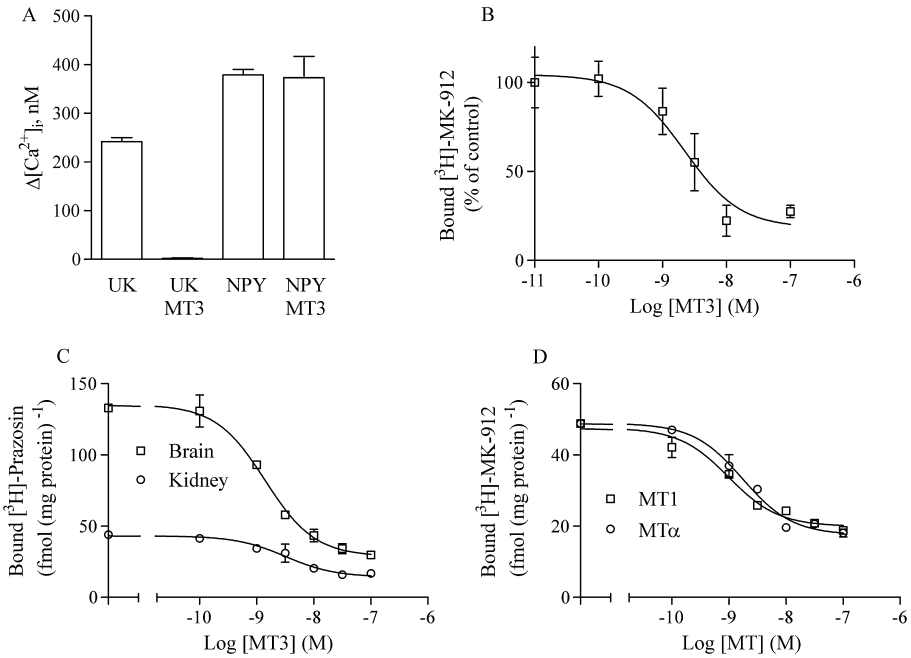

Figure 6

MT effects on native receptors. (A) HEL cells were assayed for α_{2A}-induced Ca^{2+} responses. After fura-2 loading, the cells were pre-incubated for 60 min with or without 100 nM MT3. Receptors were stimulated with either 100 nM UK-14,304 or 100 nM NPY. Data are means ± SD of two separate experiments for each column. (B) HEL cell membranes were incubated with 1 nM [^{3}H]-MK-912 and various concentrations of MT3 and the bound radioligand concentrations determined. Data points are means ± SD of two experiments with duplicate samples. (C) Rat brain and kidney membranes were incubated with 1 nM [^{3}H]-prazosin and various concentrations of MT3 and the bound radioligand concentrations determined. Data points are means ± SD of one experiment with triplicate samples. The effect of MT3 was confirmed in two additional experiments. (D) Titration of MT1 and MTα against 1 nM [^{3}H]-MK-912 in rat kidney membranes. Data points are means ± SD of one experiment with triplicate samples. The effect of the MTs was confirmed in two additional experiments.

Table 5

Sequence alignment of selected mamba toxins

	1	15	30	45	60	% Identity
MT1	LTCVTSKSIFGITTE	NCPDGQNLCFKKWYY	IVPRYSDITWGCAAT	CPKPTNVRETIRCCE	TDKCNE	100
MT4	LTCVTSKSIFGITTE	NCPDGQNLCFKKWYY	IVPRYSDITWGCAAT	CPKPTNVRETIHCCE	TDKCNE	98
MTα	LTCVTSKSIFGITTE	NCPDGQNLCFKKWYY	LNHRYSDITWGCAAT	CPKPTNVRETIHCCE	TDKCNE	94
ρ-Da1b	LTCVTKDTIFGITTQ	NCPAGQNLCFIRRHY	INHRYTEITRGCTAT	CPKPTNVRETIHCCN	TDKCNE	74
ρ-Da1a	LTCVTSKSIFGITTE	DCPDGQNLCFKRRHY	VVPKIYDSTRGCAAT	CPIPENY-DSIHCCK	TDKCNE	73
MT3	LTCVTKNTIFGITTE	NCPAGQNLCFKRWHY	VIPRYTEITRGCAAT	CPIPENY-DSIHCCK	TDKCNE	71
MT7	LTCVKSNSIWFPTSE	DCPDGQNLCFKRWQY	ISPRMYDFTRGCAAT	CPKAE-YRDVINCCG	TDKCNK	64

ability of inhibition. This could relate to the non-competitive characteristic of the toxins seen in equilibrium binding experiments, but more likely it is a consequence of the slow dissociation from the receptor that generates this type of behaviour. In general, the affinity of the toxin for a certain receptor, and thus also the dissociation rate, seems to determine whether the inhibition of fast, transient responses will behave surmountably or insurmountably. MT7 inhibits the M_1 receptor insurmountably in the same functional assay, but when part of the toxin-binding domains is exchanged the affinity drops and the inhibition becomes increasingly surmountable (Kukkonen *et al.*, 2004). Another factor that needs to be taken into account is the receptor expression level and the existence of potential receptor reserves, which is not only an artefact of recombinant expression but a phenomenon also apparent in physiological systems (Kenakin, 1984; Chong and Peachell, 1999). Here, we demonstrate with the α_{1A}-adrenoceptor that the inhibitory profile of a toxin antago-

nist is strongly affected by a receptor reserve. Such receptor reserves have also been implicated in the inhibition profile of another α_1-adrenoceptor toxin, ρ-TIA from a marine snail, on contractile responses of rat vas deferens (Sharpe *et al.*, 2003).

There have been some uncertainties regarding the effect of MT1 on the M_1 receptor. Some early reports measuring the effect of MT1 administration either *in vivo* or on tissue responses suggested an agonistic property of the toxin (Jerusalinsky *et al.*, 1995; Jolkkonen *et al.*, 1995a). In contrast, muscarinic receptor-stimulated adenylyl cyclase activity in rat frontal cortex was antagonized by MT1 without signs of agonism (Onali and Olianas, 1998). Using up to 20 μM of synthetic MT1, Servent and colleagues could not detect Ca^{2+} mobilization in M_1-transfected cells (Servent and Fruchart-Gaillard, 2009). In the present study, we used much lower concentrations of MT1 together with carbachol to assess potential allosteric enhancements of the response. However, MT1 showed only antagonistic behaviour with a similar affinity to that found previously for venomous MT1 (Mourier *et al.*, 2003). It has also been found that MT1 inhibits the noradrenaline-stimulated contraction of rabbit vas deferens (Harvey *et al.*, 2002), indicating that the anti-adrenoceptor activity of MT1 might be responsible for some of the effects seen on tissue responses.

MT3 has been well characterized on mAChRs due to its high affinity for the M_4 receptor and the high selectivity for this subtype (Jolkkonen *et al.*, 1994; Olianas *et al.*, 1996; Olianas *et al.*, 1999). We found that this toxin was rather promiscuous among the α-adrenoceptors, binding with high affinity to α_{1A}, α_{1D} and α_{2A}, and with slightly lower affinity to α_{1B} and α_{2C}. All of the high-affinity binding was found to be non-competitive, as judged by an inability to displace all radioligand. This also included the M_4 receptor where about 13% of the radiolabelled ligand remained bound at a saturating MT3 concentration (1 μM). It has previously been suggested that MT3 would bind competitively with orthosteric ligands at the M_4 receptor; this was based on complete displacement of radioligand and shifts of the K_d values for [^{3}H]-NMS measured in saturation binding in the presence of the toxin (Olianas *et al.*, 1996).

Varying the radioligand concentration in the MT3 displacement experiments also revealed an initial shift in the MT3 potency in our work. However, this competitive shift saturated at higher radioligand concentrations, indicating that the reciprocal binding of the two ligands is more complex than a simple competition. A similar lack of potency shift has also been observed previously for MT3 on the M_4 receptor (Liang *et al.*, 1996).

One of our aims was to determine whether MT3 binds in different ways to the different high-affinity targets. In the kinetic experiments measuring the toxin's influence on antagonist dissociation rates, we could not find any effect of MT3 on either receptor. In experiments analysing the functional antagonism in the same cell background, MT3 displayed quite similar inhibition profiles for all the receptors tested, with pronounced suppressions of the maximal responses. The use of short and long pre-incubations revealed that there might be some differences in the binding to different receptors. For example, the α_{2A}-adrenoceptor appeared insensitive to MT3 with short-term incubations, suggesting that some structural features in this receptor protein need to be re-arranged by the toxin in order to bind or to exert an effect on agonist action. There have been some reports on isomerization phenomena in the binding of MTs to muscarinic receptors (Toomela *et al.*, 1994; Jolkkonen *et al.*, 2001). It is possible that the toxins induce changes in the receptor conformation in order to engage more binding contacts and strengthen the binding, or alternatively to simply coerce the receptor into an inactive state in the case of antagonists.

To conclude, peptide toxins from venomous animals have mostly evolved to target specific molecules. Their specificity is probably a cause of the multiple contact sites, which together make up the total binding affinity and also preclude interactions with imperfectly matched homologous proteins. As described here, at least the MT3 toxin seems to be an exception to this specificity and should be regarded as a multi-target toxin, with cross-over activity among adrenoceptors and mAChRs. However, if the MT3 toxin uses different receptor epitopes for binding to the different receptors and by doing so also exposes structurally distinct contact points to the receptors, it might be possible to restrict the selectivity of MT3 by mutagenesis to single receptor subtypes. This will be a challenging task for the future.

Acknowledgements

We thank Drs S Uhlén and K Minneman for receptor cDNAs. We would also like to thank PM Turunen and C Aspelin for providing different cell lines and Dr A-C Engblom for help with rat preparations. This study was funded by The Academy of Finland and The Magnus Ehrnrooth Foundation.

Conflicts of interest

None.

References

Adem A, Åsblom A, Johansson G, Mbugua PM, Karlsson E (1988). Toxins from the venom of the green mamba *Dendroaspis angusticeps* that inhibit the binding of quinuclidinyl benzilate to muscarinic acetylcholine receptors. Biochim Biophys Acta 968: 340–345.

Baker JG (2005). The selectivity of beta-adrenoceptor antagonists at the human beta1, beta2 and beta3 adrenoceptors. Br J Pharmacol 144: 317–322.

Bosmans F, Tytgat J (2007). Voltage-gated sodium channel modulation by scorpion alpha-toxins. Toxicon 49: 142–158.

Bradley KN (2000). Muscarinic toxins from the green mamba. Pharmacol Ther 85: 87–109.

Bradley KN, Rowan EG, Harvey AL (2003). Effects of muscarinic toxins MT2 and MT7, from green mamba venom, on m1, m3 and m5 muscarinic receptors expressed in Chinese Hamster Ovary cells. Toxicon 41: 207–215.

Catterall WA, Cestele S, Yarov-Yarovoy V, Yu FH, Konoki K, Scheuer T (2007). Voltage-gated ion channels and gating modifier toxins. Toxicon 49: 124–141.

Caulfield MP, Birdsall NJ (1998). International Union of Pharmacology. XVII. Classification of muscarinic acetylcholine receptors. Pharmacol Rev 50: 279–290.

Cherezov V, Rosenbaum DM, Hanson MA, Rasmussen SG, Thian FS, Kobilka TS *et al.* (2007). High-resolution crystal structure of an engineered human beta2-adrenergic G protein-coupled receptor. Science 318: 1258–1265.

Chong LK, Peachell PT (1999). Beta-adrenoceptor reserve in human lung: a comparison between airway smooth muscle and mast cells. Eur J Pharmacol 378: 115–122.

Fruchart-Gaillard C, Mourier G, Marquer C, Stura E, Birdsall NJ, Servent D (2008). Different interactions between MT7 toxin and the human muscarinic M1 receptor in its free and N-methylscopolamine-occupied states. Mol Pharmacol 74: 1554–1563.

Harvey AL, Kornisiuk E, Bradley KN, Cervenansky C, Duran R, Adrover M *et al.* (2002). Effects of muscarinic toxins MT1 and MT2 from green mamba on different muscarinic cholinoceptors. Neurochem Res 27: 1543–1554.

Huang L, Wei YY, Momose-Hotokezaka A, Dickey J, Okusa MD (1996). Alpha 2B-adrenergic receptors: immunolocalization and regulation by potassium depletion in rat kidney. Am J Physiol 270: F1015–F1026.

Jansson CC, Karp M, Oker-Blom C, Näsman J, Savola JM, Åkerman KE (1995). Two human alpha 2-adrenoceptor subtypes alpha 2A-C10 and alpha 2B-C2 expressed in Sf9 cells couple to transduction pathway resulting in opposite effects on cAMP production. Eur J Pharmacol 290: 75–83.

Jerusalinsky D, Kornisiuk E, Bernabeu R, Izquierdo I, Cervenansky C (1995). Muscarinic toxins from the venom of Dendroaspis snakes with agonist-like actions. Toxicon 33: 389–397.

Jolkkonen M, van Giersbergen PL, Hellman U, Wernstedt C, Karlsson E (1994). A toxin from the green mamba Dendroaspis angusticeps: amino acid sequence and selectivity for muscarinic m4 receptors. FEBS Lett 352: 91–94.

Jolkkonen M, Adem A, Hellman U, Wernstedt C, Karlsson E (1995a). A snake toxin against muscarinic acetylcholine receptors: amino acid sequence, subtype specificity and effect on guinea-pig ileum. Toxicon 33: 399–410.

Jolkkonen M, Van Giersbergen PL, Hellman U, Wernstedt C, Oras A, Satyapan N *et al.* (1995b). Muscarinic toxins from the black mamba Dendroaspis polylepis. Eur J Biochem 234: 579–585.

Jolkkonen M, Oras A, Toomela T, Karlsson E, Järv J, Åkerman KE (2001). Kinetic evidence for different mechanisms of interaction of black mamba toxins MT alpha and MT beta with muscarinic receptors. Toxicon 39: 377–382.

Karlsson E, Jolkkonen M, Mulugeta E, Onali P, Adem A (2000). Snake toxins with high selectivity for subtypes of muscarinic acetylcholine receptors. Biochimie 82: 793–806.

Kenakin TP (1984). The classification of drugs and drug receptors in isolated tissues. Pharmacol Rev 36: 165–222.

Koivula K, Rondinelli S, Näsman J (2010). The three-finger toxin MTalpha is a selective alpha(2B)-adrenoceptor antagonist. Toxicon 56: 440–447.

Kornisiuk E, Jerusalinsky D, Cervenansky C, Harvey AL (1995a). Binding of muscarinic toxins MTx1 and MTx2 from the venom of the green mamba Dendroaspis angusticeps to cloned human muscarinic cholinoceptors. Toxicon 33: 11–18.

Kornisiuk E, Jerusalinsky D, Cervenansky C, Harvey AL (1995b). Corrigendum. Toxicon 33: 1111.

Kukkonen A, Peräkylä M, Åkerman KE, Näsman J (2004). Muscarinic toxin 7 selectivity is dictated by extracellular receptor loops. J Biol Chem 279: 50923–50929.

Kukkonen JP, Näsman J, Ojala P, Oker-Blom C, Åkerman KEO (1996). Functional properties of muscarinic receptor subtypes Hm1, Hm3 and Hm5 expressed in Sf9 cells using the baculovirus expression system. J Pharmacol Exp Ther 279: 593–601.

Kukkonen JP, Huifang G, Jansson CC, Wurster S, Cockcroft V, Savola JM *et al.* (1997). Different apparent modes of inhibition of alpha2A-adrenoceptor by alpha2-adrenoceptor antagonists. Eur J Pharmacol 335: 99–105.

Liang JS, Carsi-Gabrenas J, Krajewski JL, McCafferty JM, Purkerson SL, Santiago MP *et al.* (1996). Anti-muscarinic toxins from Dendroaspis angusticeps. Toxicon 34: 1257–1267.

Max SI, Liang JS, Potter LT (1993a). Purification and properties of m1-toxin, a specific antagonist of m1 muscarinic receptors. J Neurosci 13: 4293–4300.

Max SI, Liang JS, Potter LT (1993b). Stable allosteric binding of m1-toxin to m1 muscarinic receptors. Mol Pharmacol 44: 1171–1175.

Michel MC, Brass LF, Williams A, Bokoch GM, LaMorte VJ, Motulsky HJ (1989). Alpha 2-adrenergic receptor stimulation mobilizes intracellular Ca2+ in human erythroleukemia cells. J Biol Chem 264: 4986–4991.

Mourier G, Dutertre S, Fruchart-Gaillard C, Menez A, Servent D (2003). Chemical synthesis of MT1 and MT7 muscarinic toxins: critical role of Arg-34 in their interaction with M1 muscarinic receptor. Mol Pharmacol 63: 26–35.

Musgrave IF, Seifert R (1995). Alpha 2A-adrenoceptors mediate activation of non-selective cation channels via Gi-proteins in human erythroleukaemia (HEL) cells. No evidence for a functional role of imidazoline receptors in modulating calcium. Biochem Pharmacol 49: 187–196.

Näsman J, Jolkkonen M, Ammoun S, Karlsson E, Åkerman KE (2000). Recombinant expression of a selective blocker of M(1) muscarinic receptors. Biochem Biophys Res Commun 271: 435–439.

Nirthanan S, Gwee MC (2004). Three-finger alpha-neurotoxins and the nicotinic acetylcholine receptor, forty years on. J Pharmacol Sci 94: 1–17.

Oker-Blom C, Jansson C, Karp M, Lindqvist C, Savola JM, Vlak J *et al.* (1993). Functional analysis of the human alpha 2C-C4 adrenergic receptor in insect cells expressed by a luciferase-based baculovirus vector. Biochim Biophys Acta 1176: 269–275.

Olianas MC, Adem A, Karlsson E, Onali P (1996). Rat striatal muscarinic receptors coupled to the inhibition of adenylyl cyclase activity: potent block by the selective m4 ligand muscarinic toxin 3 (MT3). Br J Pharmacol 118: 283–288.

Olianas MC, Ingianni A, Maullu C, Adem A, Karlsson E, Onali P (1999). Selectivity profile of muscarinic toxin 3 in functional assays of cloned and native receptors. J Pharmacol Exp Ther 288: 164–170.

Olianas MC, Adem A, Karlsson E, Onali P (2004). Action of the muscarinic toxin MT7 on agonist-bound muscarinic M1 receptors. Eur J Pharmacol 487: 65–72.

Onali P, Olianas MC (1998). Identification and characterization of muscarinic receptors potentiating the stimulation of adenylyl cyclase activity by corticotropin-releasing hormone in membranes of rat frontal cortex. J Pharmacol Exp Ther 286: 753–759.

Quinton L, Girard E, Maiga A, Rekik M, Lluel P, Masuyer G *et al.* (2010). Isolation and pharmacological characterization of AdTx1, a natural peptide displaying specific insurmountable antagonism of the alpha(1A)-adrenoceptor. Br J Pharmacol 159: 316–325.

Rajagopalan N, Pung YF, Zhu YZ, Wong PT, Kumar PP, Kini RM (2007). Beta-cardiotoxin: a new three-finger toxin from Ophiophagus hannah (king cobra) venom with beta-blocker activity. FASEB J 21: 3685–3695.

Rouget C, Quinton L, Maiga A, Gales C, Masuyer G, Malosse C *et al.* (2010). Identification of a novel snake peptide toxin displaying high affinity and antagonist behaviour for the alpha(2) -adrenoceptors. Br J Pharmacol 161: 1351–1360.

Ségalas I, Roumestand C, Zinn-Justin S, Gilquin B, Ménez R, Ménez A *et al.* (1995). Solution structure of a green mamba toxin that activates muscarinic acetylcholine receptors, as studied by nuclear magnetic resonance and molecular modeling. Biochemistry 34: 1248–1260.

Servent D, Fruchart-Gaillard C (2009). Muscarinic toxins: tools for the study of the pharmacological and functional properties of muscarinic receptors. J Neurochem 109: 1193–1202.

Sharpe IA, Thomas L, Loughnan M, Motin L, Palant E, Croker DE *et al.* (2003). Allosteric alpha 1-adrenoreceptor antagonism by the conopeptide rho-TIA. J Biol Chem 278: 34451–34457.

Shuttleworth TJ, Thompson JL (1991). Effect of temperature on receptor-activated changes in [Ca2+]i and their determination using fluorescent probes. J Biol Chem 266: 1410–1414.

Toomela T, Jolkkonen M, Rinken A, Jarv J, Karlsson E (1994). Two-step binding of green mamba toxin to muscarinic acetylcholine receptor. FEBS Lett 352: 95–97.

Uhlen S, Dambrova M, Näsman J, Schioth HB, Gu Y, Wikberg-Matsson A *et al.* (1998). [3H]RS79948-197 binding to human, rat, guinea pig and pig alpha2A-, alpha2B- and alpha2C-adrenoceptors. Comparison with MK912, RX821002, rauwolscine and yohimbine. Eur J Pharmacol 343: 93–101.

Vandermeers A, Vandermeers-Piret M-C, Rathé J, Waelbroeck M, Jolkkonen M, Oras A *et al.* (1995). Purification and sequence determination of a new muscarinic toxin (MT4) from the venom of the green mamba (*Dendroaspis angusticeps*). Toxicon 33: 1171–1179.

Vassilatis DK, Hohmann JG, Zeng H, Li F, Ranchalis JE, Mortrud MT *et al.* (2003). The G protein-coupled receptor repertoires of human and mouse. Proc Natl Acad Sci USA 100: 4903–4908.

Williams TJ, Blue DR, Daniels DV, Davis B, Elworthy T, Gever JR *et al.* (1999). In vitro alpha1-adrenoceptor pharmacology of Ro 70-0004 and RS-100329, novel alpha1A-adrenoceptor selective antagonists. Br J Pharmacol 127: 252–258.